Kashf Journal of Multidisciplinary Research
Vol: 03 - Issue 01 (2026)
P-ISSN: 3007-1992 E-ISSN: 3007-200X
https://kjmr.com.pk

IN SILICO IDENTIFICATION OF PHYTOCHEMICAL INHIBITORS TARGETING MMP-9 AND IL-18 IN TAKAYASU ARTERITIS

Mehwish Majeed[1,2], Alina Sehar[2], Rabia Sajid[2,3], *Muhammad Zurgham Akram[1,2]

[1]*College of Medicine and Biological Information Engineering Northeastern University Shenyang, Liaoning, 110819, China.*
[2]*Department of Computer Science, University of Agriculture Faisalabad, Agriculture University Road, 38000, Faisalabad, Pakistan.*
[3]*College of Basic Medicine, Chongqing Medical University, China.*

[*]***Corresponding Author:*** (zurghamakram8@gmail.com)

DOI: (*https://doi.org/10.71146/kjmr819*)

Article Info

Abstract

Takayasu arteritis (TAK) is an autoimmune, inflammatory-driven, enduring, large-vessel vasculitis characterized by structural vascular stenosis and aneurysm formation. The major mediators of extracellular matrix breakdown and inflammatory signalling are matrix metalloproteinase-9 (MMP-9) and interleukin-18 (IL-18); there is a lack of systematic assessment of phytochemicals as dual inhibitors of these factors. The aim of the study was to discover phytochemical inhibitors with a dual potential of MMP-9 and IL-18, with strong binding capacity and pharmacokinetic viability to be used as a prospective therapeutic agent in TAK. A total of sixteen bioactive phytochemicals were obtained from PubChem and evaluated in silico. High-resolution crystal structures of MMP-9 (PDB: 1L6J) and IL-18 (PDB: 2VXT) were used in molecular docking. Docking identified seven top-ranking compounds, demonstrating consistently high binding affinities across both targets, stabilized through hydrogen bonding, hydrophobic interactions, and π-stacking within structurally relevant pockets. SwissADME profiling has shown favourable pharmacokinetics of conformity to Lipinski Rule of Five and high gastrointestinal absorption and appropriate bioavailability, which favour their drug-likeness. The occupancy of ligands in the functional binding cavities was confirmed by CASTp analysis. These results suggest that quercetin and luteolin might be considered as possible dual-target drugs, capable of curing inflammatory signalling and extra-cellular matrix remodelling during TAK. Future research can confirm the efficacy, pharmacodynamics, and safety of these phytochemicals in vitro and in vivo and develop them as potential therapeutics.

Keywords: *Takayasu arteritis; MMP-9, IL-18; phytochemicals; quercetin; luteolin; molecular docking; ADME profiling*

1. Introduction

Takayasu arteritis (TAK) is a rare, chronic, idiopathic large-vessel vasculitis that predominantly affects the aorta and its major branches, leading to progressive vascular stenosis, occlusion, formation of aneurysm, and ischemic complications that cause significant morbidity and mortality in the case of inappropriate treatment [1,2,3]. It disproportionately affects young women, particularly in Asian and Latin American populations, though it occurs worldwide in diverse ethnic groups [4,5,6]. Arteries in TAK have a histological appearance of granulomatous and panarteritic inflammation with transmural infiltration of $CD4^+$ and $CD8^+$ T cells, γδ T cells, macrophages, and multinucleated giant cells, leading to intimal thickening, adventitial fibrosis, disruption of elastin and collagen fibres, and structural remodelling of the vessel wall that underlies luminal narrowing and aneurysm development [7, 8]. Clinically, TAK is characterized by limb claudication, pulse deficits, blood pressure discrepancies, and symptoms of organ ischemia, and it generally follows a recurrent-remitting disease progression complicating the management and prognosis [9,10,11].

Natural phytochemicals are bioactive compounds derived from plants and have attracted considerable interest for their anti-inflammatory, antioxidant, immunomodulatory, and extracellular matrix-modulating properties, making them promising candidates for therapeutic development in chronic inflammatory and vascular diseases [12,13,14]. For example, quercetin, a ubiquitous flavonol, attenuates pro-inflammatory cytokines and matrix metalloproteinase activity in multiple preclinical models of inflammation and vascular injury, and luteolin, a flavone found in celery and parsley, suppresses IL-1β and TNF-α signalling while inhibiting extracellular matrix (ECM) related proteases in vitro [15-19]. Other plant-derived compounds, including curcumin [20], epigallocatechin-3-gallate (EGCG) [21], and hesperidin [22], also have anti-inflammatory effects through modulation of NF-κB, MAPK, and oxidative stress pathways in vascular and immune cell systems [23,24]. Together, these phytochemicals influence a variety of nodes of inflammation and matrix remodelling, suggesting potential utility in diseases where immune dysregulation and ECM breakdown are pathogenic [25,26].

Computational methods of molecular docking [27,28], binding pocket analysis [29], and ADME assessment [30] are powerful tools in early drug discovery that enable rapid evaluation of putative interactions between small molecules and protein targets [31,32,33]. Molecular docking approximates the binding affinities and interaction patterns of ligands in a particular protein active site to rank compounds with the best predicted fit, followed by ADME profiling, an evaluation of pharmacokinetic properties of solubility, membrane permeability, and drug-likeness, to reduce resource usage and then empirical testing, which speeds up the lead optimization cycle [34,35]. These in silico methods have enabled the identification of new scaffolds and repurposed compounds in the context of inflammatory and autoimmune diseases [36,37].

Recent biomarker and gene expression studies in TAK have expanded the understanding of disease mechanisms beyond conventional clinical markers such as erythrocyte sedimentation rate and C-

reactive protein [38,39]. Thorough reviews indicate that TAK biomarkers can be classified into several categories, including cytokines, chemokines, cell adhesion molecules, and matrix metalloproteinases, which are useful for early diagnosis, disease activity evaluation, and possible therapeutic decisions [40,41]. MMPs, particularly MMP-9, and pro-inflammatory cytokines such as IL-6 and IL-18 are among the most frequently investigated markers, with elevated levels associated with active disease and extensive molecular signatures identified in prospective cohort analyses following biologic therapies [42,43,44]. For example, MMP9 has been detected at significantly elevated baseline levels in TAK patients relative to controls and remains a candidate marker of vascular activity despite treatment [45,46]. On the other hand, IL-18 gene polymorphisms have been linked with angiogenesis-related pathways in TAK [47,48].

However, although IL-18 and MMP-9 are individually implicated in the inflammatory and remodelling processes of TAK [45,48], no published studies to date have systematically evaluated phytochemical inhibition against these two proteins in tandem, leaving a critical gap in translational research. Experimental work on phytochemical modulation of cytokines or MMPs tends to focus on single targets or disease models outside of TAK [47,48], and computational screenings in inflammatory diseases have not yet addressed the inhibition of both IL-18 and MMP-9 specifically. This highlights an unmet need for rational evaluation of phytochemicals as potential dual modulators of these key mediators in TAK pathogenesis.

In the present study, we aimed to address this gap by using structure-based molecular docking, binding pocket analysis, and SwissADME profiling to evaluate a panel of sixteen phytochemicals with reported anti-inflammatory potential for their ability to bind and potentially inhibit IL-18 and MMP-9 key mediators implicated in TAK and to identify lead compounds with favourable pharmacokinetic characteristics for prioritization in future experimental validation.

2. Materials and methods

2.1 Target protein structure selection

Three-dimensional (3D) crystal structures of the target proteins were retrieved from the RCSB Protein Data Bank (RCSB-PDB) based on structural integrity, resolution, and suitability for docking studies [49]. The structure of matrix metalloproteinase-9 (MMP-9) was selected as PDB ID: 1L6J, determined by X-ray diffraction with a resolution of 2.50 Å, representing the catalytic domain in a single-chain configuration appropriate for ligand interaction analysis. The structure of interleukin-18 (IL-18) was selected as PDB ID: 2VXT, also solved by X-ray diffraction, with a resolution of 1.49 Å, providing high structural accuracy for docking simulations.

2.2 Ligand molecule retrieval and selection

Sixteen phytochemicals with reported anti-inflammatory potential were curated through a literature review and retrieved from the PubChem database in SDF format [51]. The selected molecules represent multiple phytochemical classes, including flavonoids (quercetin, luteolin,

apigenin, myricetin, kaempferol, genistein), polyphenols (resveratrol, curcumin, ellagic acid), alkaloids (berberine), quinones (emodin, thymoquinone), isothiocyanates (sulforaphane), catechins (epigallocatechin gallate), and terpenoids (β-boswellic acid). These compounds were selected due to documented roles in modulating inflammatory mediators, oxidative stress pathways, or matrix-degrading enzymes.

2.3 Protein preparation

Protein preprocessing was carried out using AutoDock Tools (ADT) [50]. Crystallographic water molecules, ions, and co-crystallized ligands were removed from the protein structures to avoid interference during docking. Polar hydrogen atoms were added, and Kollman charges were assigned. The prepared protein structures were saved in PDBQT format for docking compatibility.

2.4 Ligand preparation

Ligand structures obtained in SDF format were converted to PDB format and processed using AutoDock Tools. Hydrogen atoms were added, Gasteiger charges were assigned, and rotatable bonds were defined to allow conformational flexibility. Prepared ligands were exported in PDBQT format.

2.5 Grid box configuration

The docking search space for each protein was defined using AutoDock Tools by establishing a grid box that encompassed the predicted active binding regions. For MMP-9 (PDB ID: 1L6J), the grid box was centered at coordinates (36.885, 38.845, 34.622) with dimensions of 40 × 40 × 40 Å, ensuring adequate coverage of the catalytic and substrate-binding domain. For IL-18 (PDB ID: 2VXT), the grid center was set to (32.025, - 9.402, -5.442) with the same grid dimensions of 40 × 40 × 40 Å to encompass the primary ligand-interaction region. An exhaustiveness value of 8 was applied in both docking runs to balance computational efficiency and conformational sampling. These parameters ensured that the docking algorithm explored all plausible ligand orientations within structurally relevant binding pockets.

2.6 Molecular docking

Docking simulations were performed using AutoDock Vina with default scoring parameters. The algorithm explored ligand conformations and orientations within the defined grid boxes and estimated binding affinity as predicted free energy of binding (kcal/mol). For each protein-ligand pair, the best pose with the lowest binding energy was selected.

2.7 Selection of optimal binding conformations

Docked complexes were ranked according to binding affinity, where more negative binding energies indicated stronger predicted interactions. Top-scoring conformations for each compound were selected for detailed interaction analysis.

2.8 Protein-ligand interaction analysis

Top docking poses were visualized using BIOVIA Discovery Studio Visualizer [52] to identify hydrogen bonds, hydrophobic interactions, π–π stacking, and electrostatic contacts between ligands and protein residues. Three-dimensional visualization and surface hydrophobicity assessment were performed using UCSF Chimera 1.19 [53].

2.9 Post-docking comparative analysis

Seven compounds that showed superior docking scores (hesperidin, quercetin, luteolin, apigenin, myricetin, beta-boswellic acid, and genistein) were further analyzed for 2D/3D interaction profiles and binding stability to compare interaction patterns across both targets.

2.10 ADME and drug-likeness profiling

Pharmacokinetic properties were predicted using SwissADME [54]. Evaluated parameters included Lipinski's Rule of Five, gastrointestinal absorption, water solubility (logS), blood-brain barrier permeability, skin permeation (logKp), CYP450 inhibition profiles, TPSA, and bioavailability score. Compounds with favourable ADME characteristics and minimum rule violations were prioritized.

2.11 Lead compound selection

Based on an integrated assessment of docking energy, interaction stability, and ADME performance, quercetin and luteolin were identified as the most promising lead compounds for potential inhibition of MMP-9 and IL-18 and selected for further consideration.

2.12 Binding pocket analysis

Binding pocket prediction was performed using CASTp to predict and validate active site cavities of MMP-9 and IL-18 [55]. Pocket surface area and volume were analyzed to confirm that docking simulations targeted structurally relevant regions.

3. Results and discussion

The current investigation aimed to identify potential phytochemical compounds capable of binding to MMP-9 and IL-18, two key biomarkers involved in inflammatory remodelling and tumour-associated microenvironment regulation, and to evaluate their potential as natural inhibitors with help of molecular docking and in silico ADME predictions. These proteins were selected due to their established roles in extracellular matrix degradation, immune modulation, and disease progression. In this study, 16 phytochemicals previously reported to possess anti-inflammatory, antioxidant, and anticancer activities were examined to explore their inhibitory potential against these molecular targets.

3.1 Retrieval of target structures and ligand molecules

The crystallographic structures of IL-18 (PDB ID: 2VXT) and MMP-9 (PDB ID: 1L6J) were retrieved and prepared for docking by removing water molecules and heteroatoms, followed by energy minimization.

Table 1. List of phytochemicals and their molecular properties, selected on the basis of reported anti-inflammatory and vascular protective potential for evaluation as MMP-9 and IL-18 inhibitors

Phytochemicals	Molecular formula	Molecular weight(g/mol)	PubChem ID
Berberine	$C_{20}H_{18}NO_{4+}$	336.4	2353
Emodin	$C_{15}H_{10}O_5$	270.24	3220
Sulforaphane	$C_6H_{11}NOS_2$	177.3	5350
Thymoquinone	$C_{10}H_{12}O_2$	164.2	10281
Hesperidin	$C_{28}H_{34}O_{15}$	610.6	10621
Epigallocatechin gallate	$C_{22}H_{18}O_{11}$	458.4	65064
Beta-boswellic acid	$C_{30}H_{48}O_3$	456.7	168928
Resveratol	$C_{14}H_{12}O_3$	228.24	445154
Curcumin	$C_{21}H_{20}O_6$	368.4	969516
Quercetin	$C_{15}H_{10}O_7$	302.23	5280343
Apigenin	$C_{15}H_{10}O_5$	270.24	5280443
Luteolin	$C_{15}H_{10}O_6$	286.24	5280445
Kaempferol	$C_{15}H_{10}O_6$	286.24	5280863
Genistein	$C_{15}H_{10}O_5$	270.24	5280961
Myricetin	$C_{15}H_{10}O_8$	318.23	5281672
Ellagic acid	$C_{14}H_6O_8$	302.19	5281855

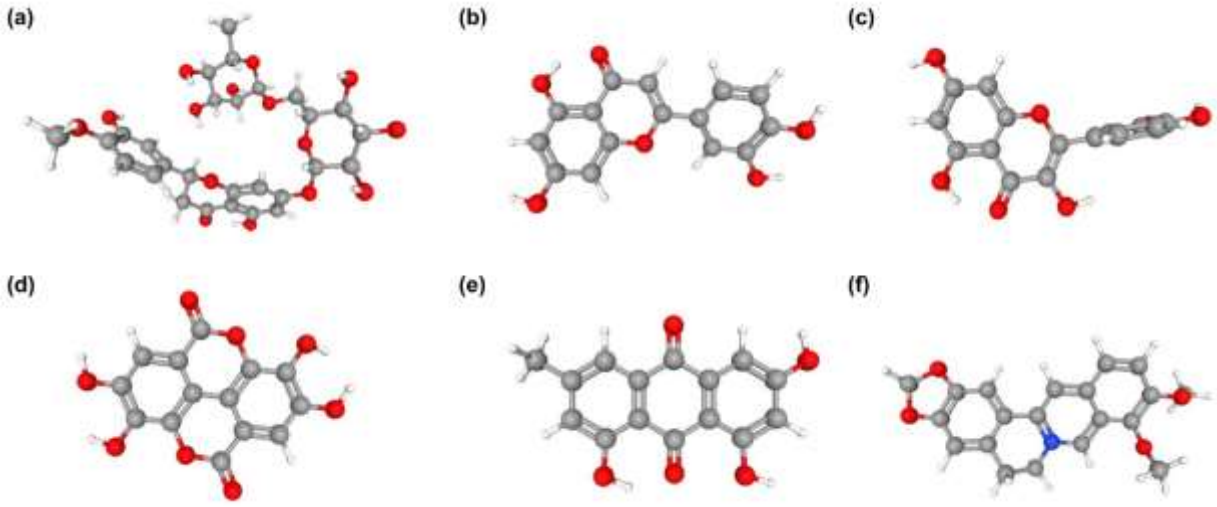

Fig. 1. Three-dimensional SDF structures of some phytochemicals obtained from PubChem database: (a) Hesperidin (b) Luteolin (c) Quercetin (d) Ellagic Acid (e) Emodin (f) Berberine

3.2 Phytochemical library construction and characterization

A dataset comprising 16 bioactive phytochemicals with reported pharmacological relevance, including flavonoids, phenolic acids, and plant-derived polyphenols, was constructed (Table 1). These compounds are widely recognized for their free radical scavenging, anti-inflammatory, and enzyme-modulating properties. Their 3D conformations were obtained in SDF format from the PubChem (see Fig. 1) database and converted into PDBQT format for docking analysis.

3.3 Protein-ligand docking analysis

Molecular docking was conducted between 16 phytochemicals and two target proteins, MMP-9 (1L6J) and IL-18 (2VXT), generating 32 protein-ligand complexes. Docking scores, hydrogen bond interactions, and binding conformations were analyzed to evaluate interaction stability. Binding affinities ranged from -3.8 to -9.9 kcal/mol, indicating diverse interaction strengths among compounds (Table 2). Flavonoid compounds demonstrated the strongest binding performance. The highest affinity toward MMP-9 was observed for luteolin (-9.9 kcal/mol), followed by quercetin (-9.6 kcal/mol) and apigenin (-9.6 kcal/mol). For IL-18, the strongest interaction was shown by hesperidin (-8.6 kcal/mol), followed by β-boswellic acid (-8.1 kcal/mol) and myricetin (-7.8 kcal/mol). Molecules with more negative docking scores exhibited stronger predicted binding, suggesting higher inhibitory potential.

Table 2. Docking binding affinities of phytochemicals against MMP9 and IL-18

Compounds	IL-18/2vxt affinity (kcal/mol)	MMP-9/1l6j affinity (kcal/mol)
Berberine	-7.6	-7.8
Emodin	-7.3	-8.6
Sulforaphane	-3.8	-5
Thymoquinone	-5.3	-6.6
Hesperidin	-8.6	-9
Epigallocatechin gallate	-7.4	-7.9
Beta-boswellic acid	-8.1	-8.4
Resveratol	-6.4	-8.3
Curcumin	-6.6	-7.3
Quercetin	-7.9	-9.6
Apigenin	-7.2	-9.6
Luteolin	-7.6	-9.9
Kaempferol	-6.9	-9.2
Genistein	-7	-9.3
Myricetin	-7.8	-8.8
Ellagic acid	-6.9	-8.9

3.4 Selection of top phytochemicals based on docking

Compounds were ranked based on average binding affinity across both proteins, ligand efficiency, and interaction stability. Seven phytochemicals demonstrated consistent multi-target activity which includes Hesperidin (-8.6 / -9.0), Quercetin (-7.9 / -9.6), Luteolin (-7.6 / -9.9), Apigenin (-7.2 / -9.6), Myricetin (-7.8 / -8.8), β-Boswellic acid (-8.1 / -8.4) and Genistein (-7.0 / -9.3) kcal/mol for both proteins (Table 3). Among them, Hesperidin showed the best IL-18 affinity, Luteolin exhibited the strongest MMP-9 inhibition, and Quercetin displayed balanced dual inhibition. These compounds formed hydrogen bonds and π-π interactions with active site residues, stabilizing the complexes. Detailed 2D and 3D interaction diagrams of the top seven compounds docked with protein IL-18 are shown in Fig. 2 and 3, illustrating different hydrogen bonding networks, π-interactions stabilizing the complexes and spatial orientation. Fig. 4 and Fig. 5 illustrate the 2D and 3D interaction diagrams of the top seven compounds docked with protein MMP-9, describing the spatial orientation, conformational fit, and different hydrogen and π bonds.

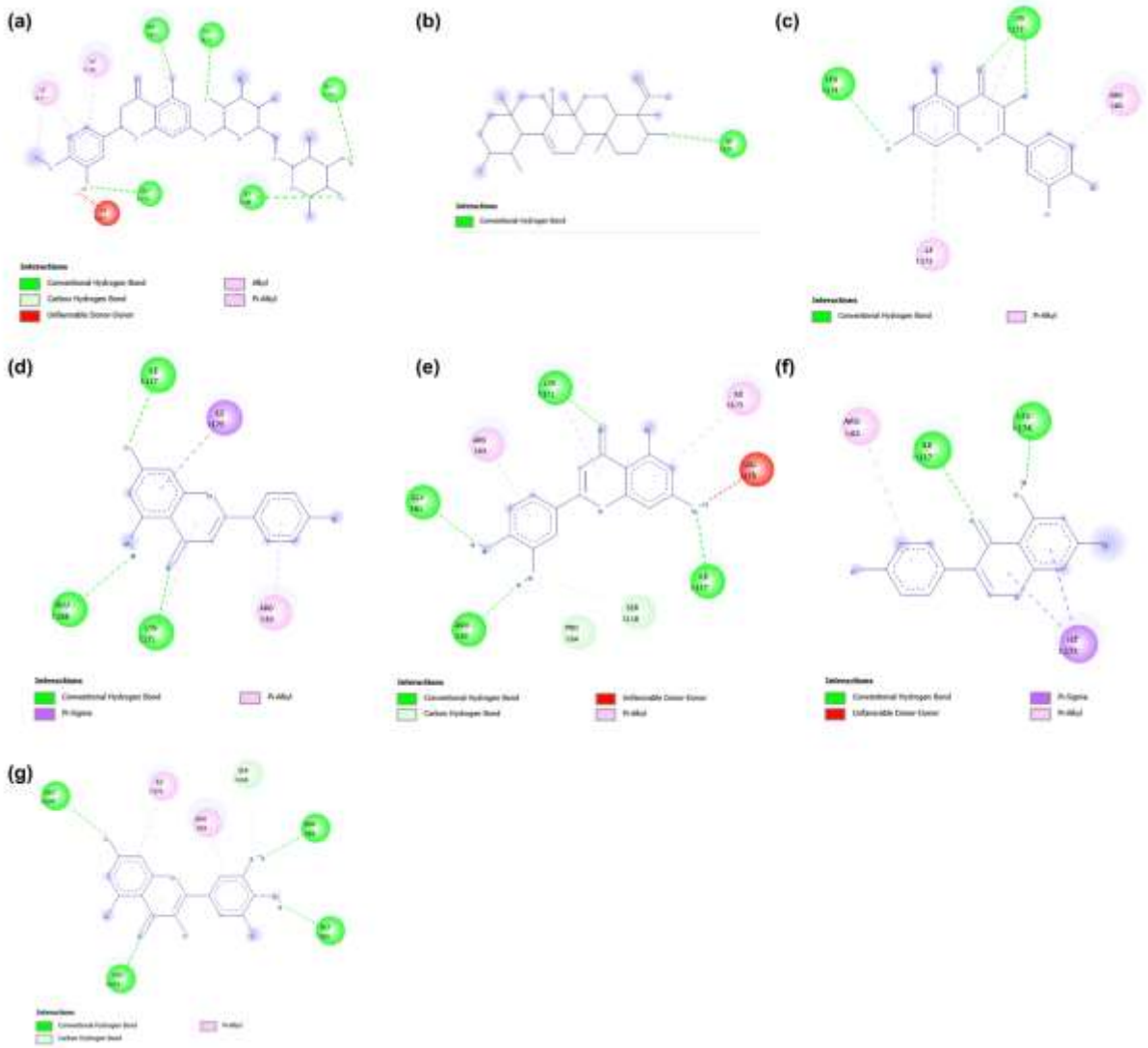

Fig. 2. 2D protein-ligand interaction diagrams illustrating the binding conformations of the seven top-ranked phytochemicals within the active site of IL-18. The maps depict conventional and carbon-hydrogen bonding, and π-alkyl/π-sigma interactions stabilizing the complexes: (a) Hesperidin, (b) Beta-Boswellic acid, (c) Quercetin, (d) Apigenin, (e) Luteolin, (f) Genistein, and (g) Myricetin

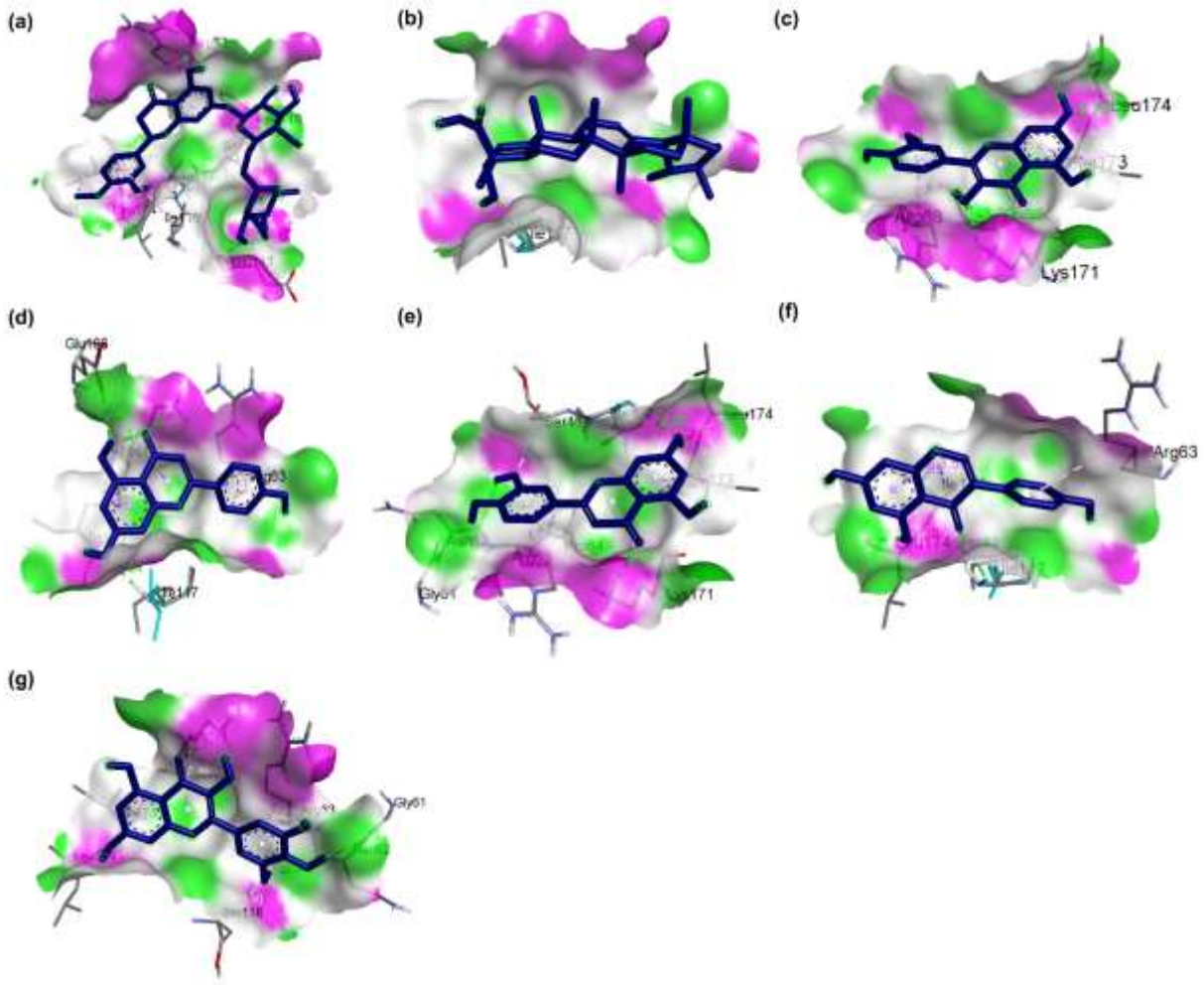

Fig. 3. 3D binding interaction models showing the spatial orientation and conformational fit of the seven highest-ranked phytochemicals inside the IL-18 binding pocket. Surface representation of the protein and ligand positioning highlights pocket occupancy and interaction stability: (a) Hesperidin, (b) Beta-Boswellic acid, (c) Quercetin, (d) Apigenin, (e) Luteolin, (f) Genistein, and (g) Myricetin

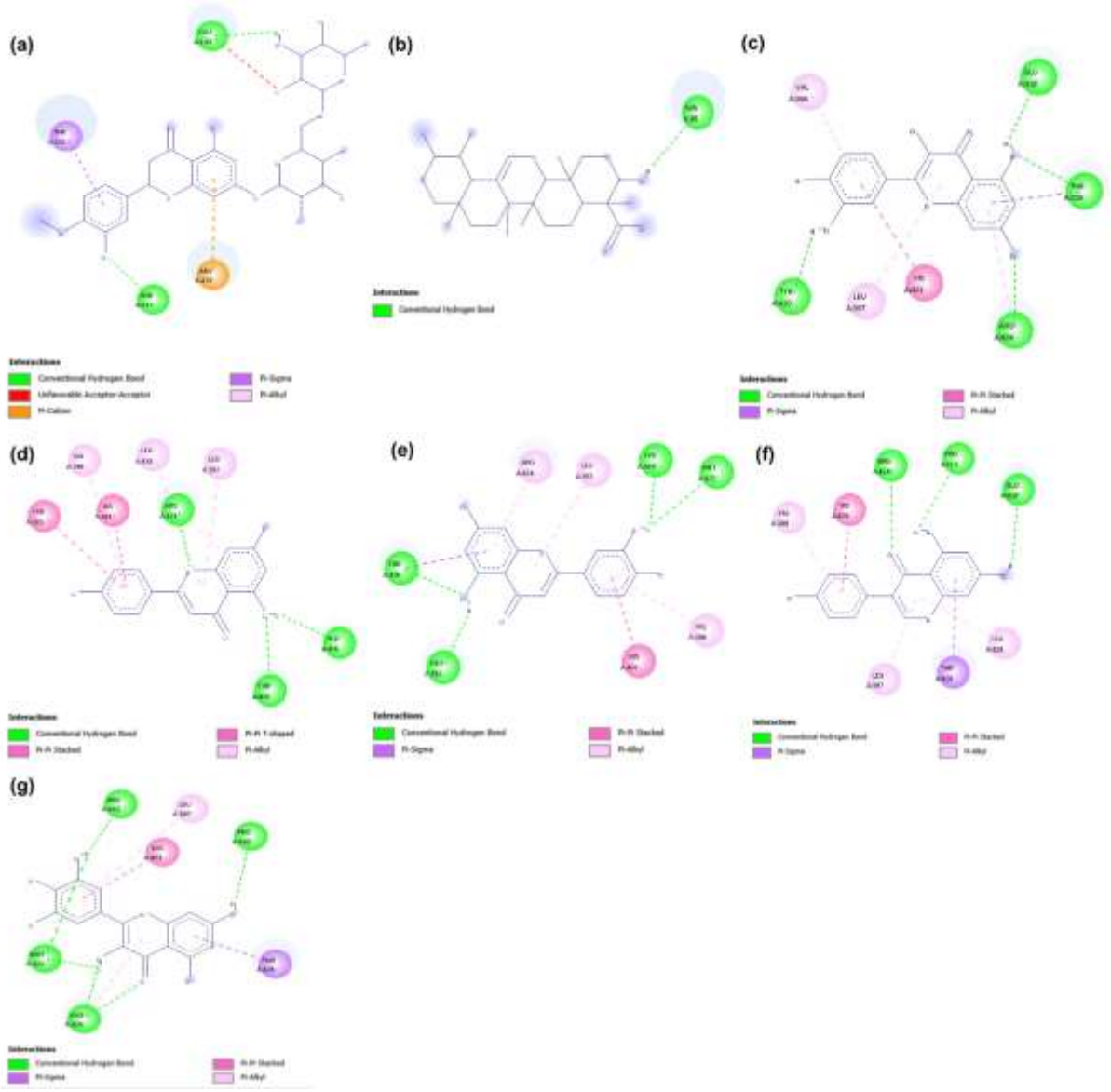

Fig. 4. 2D protein-ligand interaction schematics showing the binding poses of the seven highest-ranked phytochemicals within the catalytic site of MMP-9. The diagrams illustrate conventional hydrogen bonds along with hydrophobic and π-related interactions (π-alkyl, π-sigma, π-cation, π-stacking, and π–π contacts) that contribute to complex stabilization: (a) Hesperidin, (b) Beta-Boswellic acid, (c) Quercetin, (d) Apigenin, (e) Luteolin, (f) Genistein, and (g) Myricetin

Table 3. Docking-selected seven phytochemicals and their predicted inhibitory affinities against IL-18 and MMP-9

Compounds	IL-18 (2VXT)	MMP-9 (1L6J)	Average
Hesperidin	-8.6	-9	-8.8

Quercetin	-7.9	-9.6	-8.75
Luteolin	-7.6	-9.9	-8.75
Apigenin	-7.2	-9.6	-8.4
Myricetin	-7.8	-8.8	-8.3
Beta-boswellic acid	-8.1	-8.4	-8.25
Genistein	-7	-9.3	-8.15

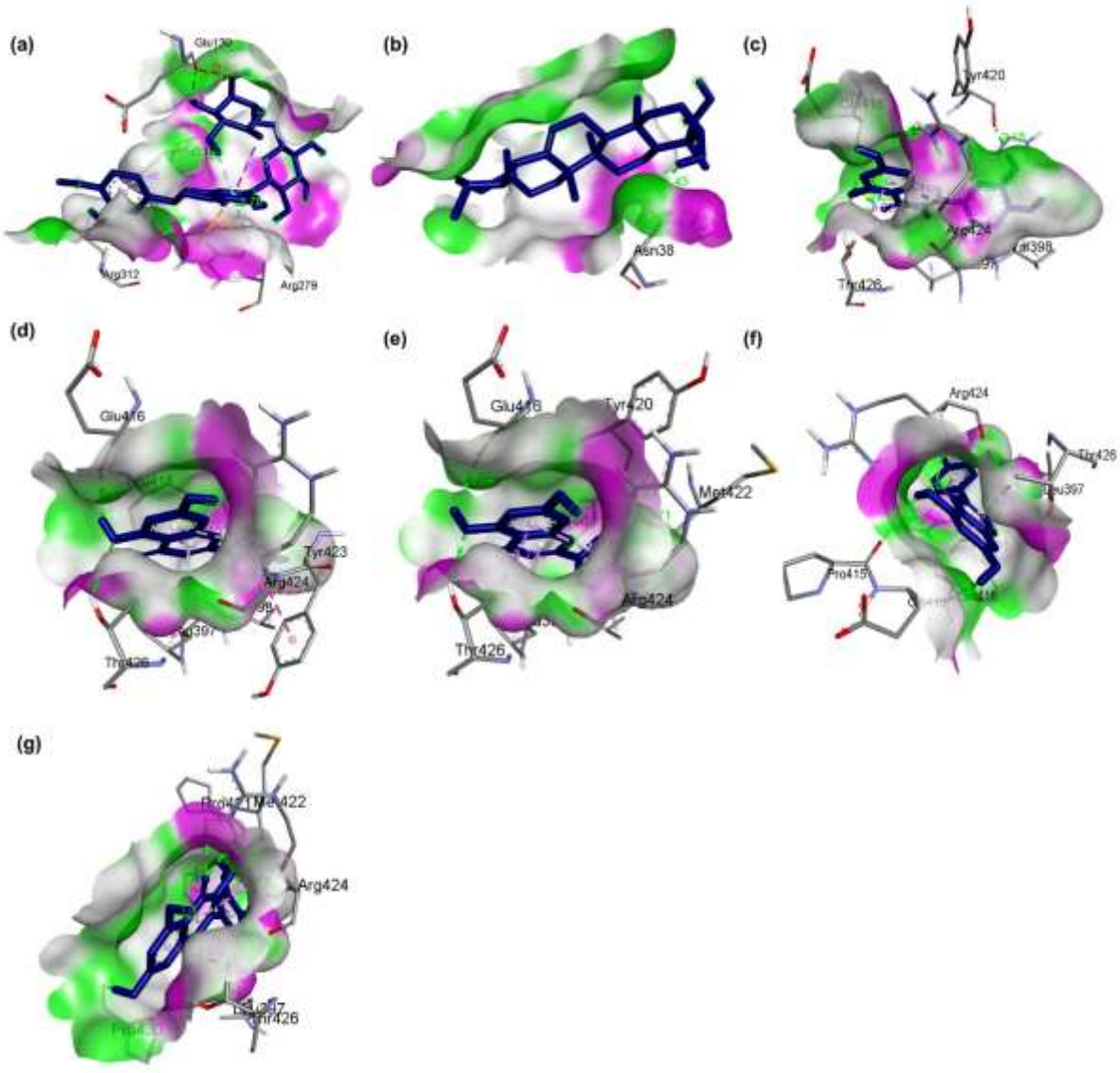

Fig. 5. 3D molecular interaction models depicting the spatial orientation and conformational accommodation of the seven top-ranked phytochemicals within the MMP-9 binding cavity. Protein

surface rendering and ligand positioning emphasize binding pocket occupancy and overall interaction stability: (a) Hesperidin, (b) β-Boswellic acid, (c) Quercetin, (d) Apigenin, (e) Luteolin, (f) Genistein, and (g) Myricetin

3.5 ADME and drug-likeness evaluation

To evaluate the pharmacokinetic feasibility of the top-ranked phytochemicals, in silico ADME profiling was performed using SwissADME. Drug-likeness was evaluated using Lipinski's Rule of Five, which states that optimal oral drugs typically have a molecular weight < 500 Da, LogP < 5, H-bond donors ≤ 5 and H-bond acceptors ≤ 10. Quercetin and luteolin were the most favourable compounds among the seven selected compounds in terms of pharmacokinetic profiles. Both molecules satisfied Lipinski's Rule of Five without any violations, i.e., maintaining molecular weights below 500 Da (quercetin 302.24 Da; luteolin 286.24 Da), hydrogen bond donors ≤ 5, and hydrogen bond acceptors within acceptable limits. Their TPSA values (131.36 Å² for quercetin and 111.13 Å² for luteolin) indicate sufficient polarity for solubility while still permitting membrane permeability. These values lie within the range associated with efficient intestinal absorption, consistent with their predicted high GI absorption. Their bioavailability scores of 0.55 further prove its suitability for oral drug development (Table 4).

Table 4. ADME evaluation and drug-likeness properties of the seven top-ranked phytochemicals selected from docking against IL-18 and MMP-9

Properties	Hesperidin	Quercetin	Luteolin	Apigenin	Myricetin	Beta-boswellic acid	Genistein
Molecular weight	610.56	302.24	286.24	270.24	318.24	456.7	270.24
Number of H-bond acceptors	15	7	6	5	8	3	5
Number of H-bond donors	8	5	4	3	6	2	3
Water solubility (logS)	-3.28	-3.16	-3.71	-3.94	-3.01	-7.81	-3.72
TPSA (A2)	234.29	131.36	111.13	90.9	151.59	57.53	90.9
Molar refractivity	141.41	78.03	76.01	73.99	80.06	136.91	73.99
Log kp (skin permeation) cm/s	-10.12	-7.05	-6.25	-5.8	-7.4	-3.22	-6.05
Bioavailability score	0.17	0.55	0.55	0.55	0.55	0.85	0.55
GI absorption	low	high	high	high	low	low	high
Lipinski rule	no	yes	yes	yes	yes	yes	yes

Blood-brain barrier (BBB)	no	no	no	no	no	no	no
CYP3A4 inhibition	no	yes	yes	yes	yes	no	yes
CYP2C9 inhibition	no	no	no	no	no	yes	no
CYP2D6 inhibition	no	yes	yes	yes	no	no	yes
CYP2C19 inhibition	no	no	no	no	no	no	no
CYP1A2 inhibition	no	yes	yes	yes	yes	no	yes

In contrast, hesperidin, although it showed strong docking performance, still has pharmacokinetic limitations, including a high molecular weight (610.56 Da), elevated TPSA (234.29 Å²), and low GI absorption, which, as a result, may limit systemic bioavailability. Beta-boswellic acid exhibited acceptable Lipinski compliance but demonstrated poor predicted solubility of logS -7.81 and low GI absorption, indicating the challenges in formulation. Myricetin, while active, showed higher polarity (TPSA 151.59 Å²), but compared to quercetin and luteolin, showed potentially reduce passive membrane permeability.

Predictions of cytochrome P450 interaction showed that quercetin and luteolin might be CYP3A4, CYP2D6, and CYP1A2 isoform inhibitors, which implicated a potential existence of metabolic interactions that would have to be experimentally assessed. However, none of the compounds were predicted to cross the blood-brain barrier, reducing the risk of central nervous system-related side effects. Skin permeation values (log Kp) results also indicate low transdermal penetration, consistent with their intended systemic anti-inflammatory role. On the whole, the results of the ADME analysis indicated that although multiple phytochemicals demonstrated high docking affinities, quercetin and luteolin were the only phytochemicals to have a strong dual-target binding with balanced physicochemical and pharmacokinetic properties, supporting their selection as the most promising lead candidates.

3.6 Binding pocket analysis

Binding pocket analysis was performed by CASTp, which identified four major cavities in both MMP-9 and IL-18 proteins, highlighting structurally relevant ligand-binding regions. In MMP-9, Pocket 1 (841.248 Å², 1233.188 Å³) encompassed the catalytic cleft, while Pocket 2 (706.935 Å², 579.364 Å³) corresponded to the substrate-binding groove; quercetin and luteolin predominantly occupied these pockets, forming hydrogen bonds, hydrophobic contacts, and π-stacking interactions. For IL-18, Pocket 1 with area 1459.496 Å² and volume 2252.146 Å³ showing a broad functional interface, with the top ligands binding stably within this cavity. These results confirm that ligand interactions occurred within structurally meaningful and potential regions, supporting the docking outcomes. Pocket metrics are summarized in Table 5, and three-dimensional visualizations are shown in Fig. 6 (MMP-9) and Fig. 7 (IL-18).

Table 5. CASTp-predicted active site pockets of MMP-9 and IL-18 with surface area and volume

Proteins	Pocket ID	Area (SA) (Å2)	Volume (SA) (Å3)
MMP-9	1	841.248	1233.188
	2	706.935	579.364
	3	136.772	123.111
	4	161.108	88.097
1L-18	1	1459.496	2252.146
	2	155.962	179.752
	3	159.174	164.159
	4	77.662	40.293

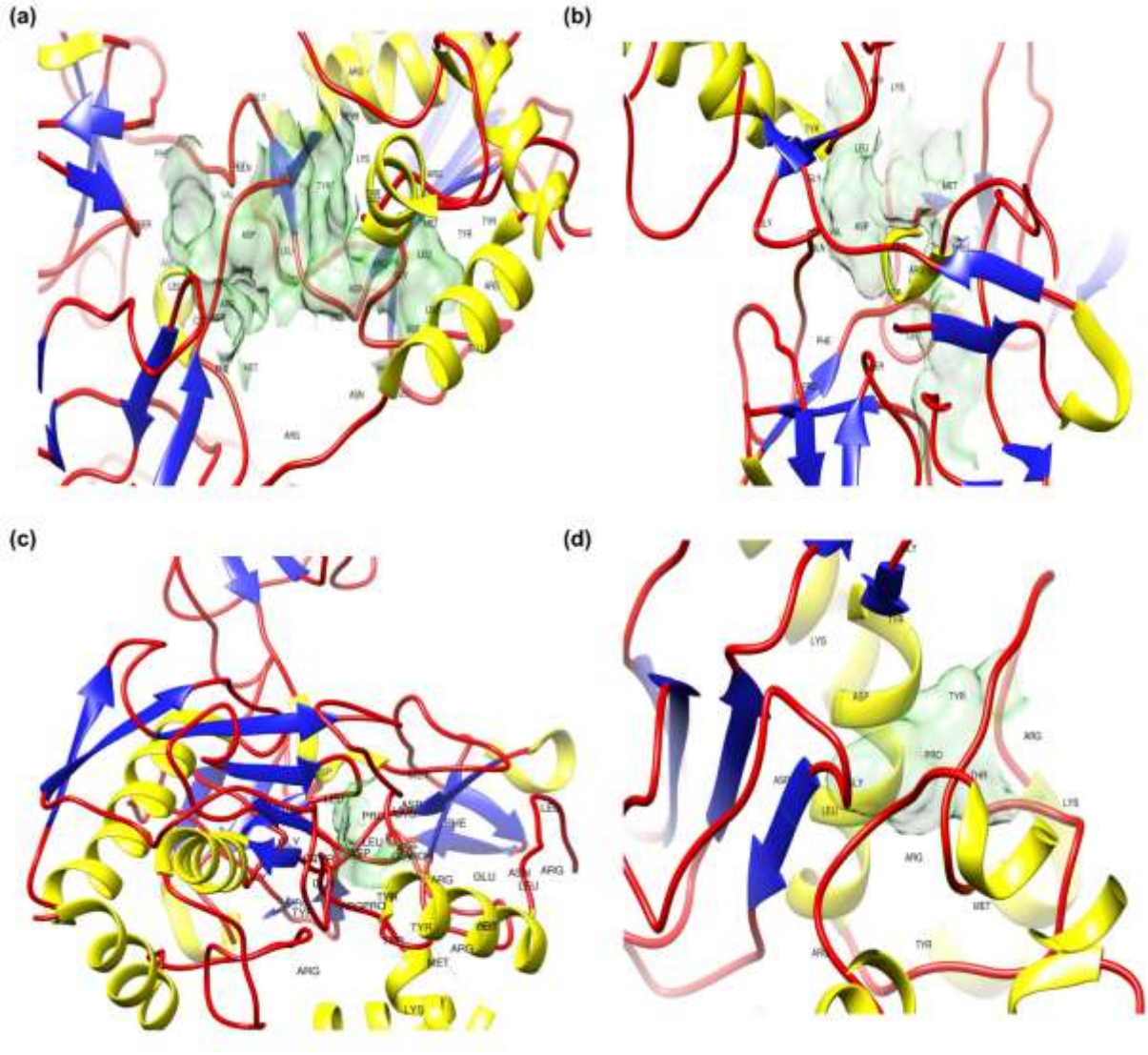

Fig. 6. 3D surface representation of the binding pocket architecture of MMP-9 predicted using CASTp. The four major pockets are illustrated as (a) Pocket 1, (b) Pocket 2, (c) Pocket 3, and (d)

Pocket 4, showing their spatial distribution, cavity depth, and potential ligand-accessible regions within the catalytic domain.

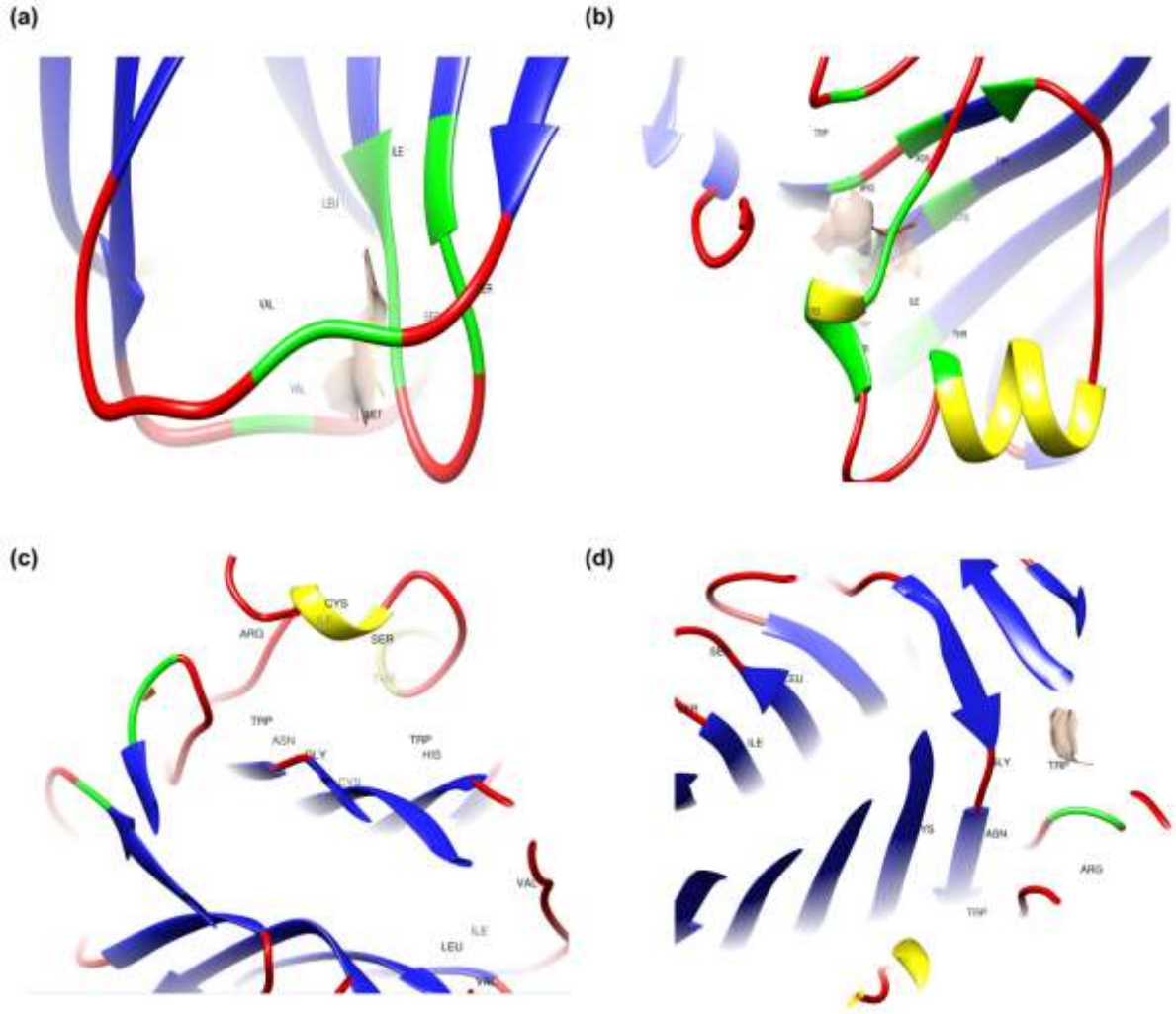

Fig. 7. 3D surface visualization of IL-18 binding pockets identified by CASTp analysis. The four principal cavities are labelled as (a) Pocket 1, (b) Pocket 2, (c) Pocket 3, and (d) Pocket 4, demonstrating the spatial distribution and volume of the principal cavities, indicating the dominant ligand-binding region involved in stabilizing phytochemical interactions.

3.7 Interpretation and future directions

The current study identified quercetin and luteolin as the most promising phytochemical inhibitors targeting MMP-9 and IL-18. These proteins demonstrated consistently high binding affinities across both target (-7.9 to -9.9 kcal/mol), favourable ligand-protein interaction profiles, and stable docking conformations, further supported by hydrogen bonding, hydrophobic interactions, and π-stacking networks. ADME evaluation reinforced their drug-likeness, high gastrointestinal absorption, and compliance with Lipinski's Rule of Five, distinguishing them from other high-affinity compounds. Lastly, Binding pocket analysis confirmed that these compounds localized

within the structurally and functionally relevant cavities of both proteins. Taken together, these findings suggest that quercetin and luteolin may serve as dual-target modulators, capable of attenuating inflammatory signalling and matrix remodelling simultaneously for Takayasu arteritis. Nevertheless, it is important to acknowledge that due to financial constraints, these results are derived from in silico docking and ADME predictions and the study is not extended to molecular dynamics simulations. Future in vitro and in vivo experimental validation is required to confirm binding stability, pharmacodynamics, and safety profiles.

4. Conclusion

This in silico study identified quercetin and luteolin as promising phytochemical inhibitors targeting both MMP-9 and IL-18, supported by strong predicted binding affinities, favourable pharmacokinetic properties, and mechanistic plausibility based on existing literature. These compounds may represent dual-target therapeutic leads in the context of chronic vascular inflammation, such as Takayasu arteritis, where current treatment options remain limited. Furthermore, these findings provide a compelling basis for exploring natural flavonoids as an adjunctive or alternative therapy option for targeting multiple disease-relevant pathways. Future investigations integrating computational and experimental approaches could facilitate the development of safe and effective phytochemical-based interventions for TAK and other inflammatory vascular disorders.

Conflicts of Interest: The authors declare no conflict of interest.

Data availability: Structural and ligand data were obtained from PDB and PubChem. Processed data are available from the corresponding author upon request.

Acknowledgement: None

References

1. Bhandari S, Butt SR, Ishfaq A, Attallah MH, Ekhator C, Nagaraj RH, Mulmi A, Kamran M, Karski A, Vargas KI, Lazarevic S. Pathophysiology, diagnosis, and management of Takayasu arteritis: a review of current advances. Cureus. 2023 Jul 29;15(7): e42667.
2. Misra DP, Singh K, Rathore U, Kavadichanda CG, Ora M, Jain N, Agarwal V. Management of Takayasu arteritis. Best Practice & Research Clinical Rheumatology. 2023 Mar 1;37(1):101826.
3. Moisii P, Jari I, Naum AG, Butcovan D, Tinica G. Takayasu's arteritis: A special case report and review of the literature. Medicina. 2024 Mar 9;60(3):456.
4. Vieira M, Ochtrop ML, Sztajnbok F, Elias CS, Verztman JF, Bica BE, Ciconelli RM, de Souza AW. The epidemiology of Takayasu arteritis in Rio de Janeiro, Brazil: a large population-based study. JCR: Journal of Clinical Rheumatology. 2023 Aug 1;29(5): e100-3.
5. Niranjan KC, Kumar SP, Lalita B, Ishwari P, Kumar YM. A rare case presentation of Takayasu arteritis affecting the bilateral common carotid arteries: a case report. Annals of Medicine and Surgery. 2025 Apr 1;87(4):2494-9.
6. Trinidad B, Surmachevska N, Lala V. Takayasu arteritis. InStatPearls [Internet] 2023 Aug 8. Stat Pearls Publishing.
7. Vaideeswar P, Deshpande JR. Pathology of Takayasu arteritis: a brief review. Annals of Pediatric Cardiology. 2013 Jan 1;6(1):52-8.
8. Li T, Gao N, Cui W, Zhao L, Du J, Shi X, Zhu J, Qiao Z, Guo S, Pan L. The role of CD8+ Granzyme B+ T cells in the pathogenesis of Takayasu's arteritis. Clinical Rheumatology. 2022 Jan;41(1):167-76.
9. Dammacco F, Cirulli A, Simeone A, Leone P, Pulli R, Angiletta D, Rubini G, Di Palo A, Vacca A, Dammacco R. Takayasu arteritis: a cohort of Italian patients and recent pathogenetic and therapeutic advances. Clinical and Experimental Medicine. 2021 Feb;21(1):49-62.
10. Aeschlimann FA, Twilt M, Yeung RS. Childhood-onset Takayasu arteritis. European Journal of Rheumatology. 2020 Feb;7(Suppl 1): S58.
11. Asongtia TE, Fomekong TG, Somo LJ, Ghislain FS, Irene KF, Edmond T. Navigating Diagnostic Delays: A Case of Takayasu Arteritis Complicated by Acute Heart Failure and Vascular Compromise in a 37-Year-Old Woman from Cameroon. Cureus. 2025 Apr 27;17(4).
12. Altemimi A, Lakhssassi N, Baharlouei A, Watson DG, Lightfoot DA. Phytochemicals: Extraction, isolation, and identification of bioactive compounds from plant extracts. Plants. 2017 Sep 22;6(4):42.
13. Ingle KP, Deshmukh AG, Padole DA, Dudhare MS, Moharil MP, Khelurkar VC. Phytochemicals: Extraction methods, identification and detection of bioactive compounds from plant extracts. Journal of Pharmacognosy and Phytochemistry. 2017;6(1):32-6.
14. Paul JK, Azmal M, Haque AS, Talukder OF, Meem M, Ghosh A. Phytochemical-mediated modulation of signaling pathways: a promising avenue for drug discovery. Advances in Redox Research. 2024 Dec 1; 13:100113.

15. Alharbi HO, Alshebremi M, Babiker AY, Rahmani AH. The role of quercetin, a flavonoid in the management of pathogenesis through regulation of oxidative stress, inflammation, and biological activities. Biomolecules. 2025 Jan 20;15(1):151.
16. Al-Khayri JM, Sahana GR, Nagella P, Joseph BV, Alessa FM, Al-Mssallem MQ. Flavonoids as potential anti-inflammatory molecules: A review. Molecules. 2022 May 2;27(9):2901.
17. Aleebrahim-Dehkordi E, Soveyzi F, Arian AS, Hamedanchi NF, Hasanpour-Dehkordi A, Rafieian-Kopaei M. Quercetin and its role in reducing the expression of pro-inflammatory cytokines in osteoarthritis. Anti-Inflammatory & Anti-Allergy Agents in Medicinal Chemistryrrent Medicinal Chemistry-Anti-Inflammatory and Anti-Allergy Agents). 2022 Sep 1;21(3):153-65.
18. Smith F. Deeper Inflammation: Examples of Extracellular Matrix Involvement and Treatment. InThe Extracellular Matrix in Health and Disease: Naturopathic Approaches to Improve Structure and Function 2025 Jul 31 (pp. 121-160). Cham: Springer Nature Switzerland.
19. Jasrotia S, Gupta S, Kudipady ML, Puttaiahgowda YM. Advancing food preservation with quercetin-based Nanocomposites: Antimicrobial, antioxidant, and controlled-release strategies-A review. Current Research in Food Science. 2025 Aug 9:101159.
20. Lan X, Liu Y, Wang L, Wang H, Hu Z, Dong H, Yu Z, Yuan Y. A review of curcumin in food preservation: Delivery system and photosensitization. Food Chemistry. 2023 Oct 30; 424:136464.
21. Song X, Du J, Zhao W, Guo Z. Epigallocatechin-3-gallate (EGCG): mechanisms and the combined applications. Combinatorial Chemistry & High Throughput Screening. 2017 Dec 1;20(10):872-85.
22. Xiong H, Wang J, Ran Q, Lou G, Peng C, Gan Q, Hu J, Sun J, Yao R, Huang Q. Hesperidin: A therapeutic agent for obesity. Drug design, development and therapy. 2019 Nov 12:3855-66.
23. Olędzka AJ, Czerwińska ME. Role of plant-derived compounds in the molecular pathways related to inflammation. International Journal of Molecular Sciences. 2023 Feb 28;24(5):4666.
24. Nakadate K, Ito N, Kawakami K, Yamazaki N. Anti-Inflammatory Actions of Plant-Derived Compounds and Prevention of Chronic Diseases: From Molecular Mechanisms to Applications. International Journal of Molecular Sciences. 2025 May 28;26(11):5206.
25. Liang D, Liu L, Zhao Y, Luo Z, He Y, Li Y, Tang S, Tang J, Chen N. Targeting extracellular matrix through phytochemicals: a promising approach of multi-step actions on the treatment and prevention of cancer. Frontiers in Pharmacology. 2023 Jul 25; 14:1186712.
26. Zheng Z, Gao J, Ma Y, Hou X. Cellular and Molecular Mechanisms of Phytochemicals Against Inflammation-Associated Diseases and Viral Infection. Cell Biology International. 2025 Jun;49(6):606-33.
27. Morris GM, Lim-Wilby M. Molecular docking. In Molecular modeling of proteins 2008 Jul (pp. 365-382). Totowa, NJ: Humana Press.

28. Paggi JM, Pandit A, Dror RO. The art and science of molecular docking. Annual review of biochemistry. 2024 Aug 2;93(1):389-410.
29. Stank A, Kokh DB, Fuller JC, Wade RC. Protein binding pocket dynamics. Accounts of chemical research. 2016 May 17;49(5):809-15.
30. Lakka NS, Kuppan C, Vadagam N, Ravinathan P, Chepuri K, Chinnakadoori SR. Molecular docking, in-vitro anticancer evaluation and ADME profiling of 7-Oxo Midostaurin. Journal of molecular structure. 2023 Dec 5; 1293:136159.
31. Lin X, Li X, Lin X. A review on applications of computational methods in drug screening and design. Molecules. 2020 Mar 18;25(6):1375.
32. Naithani U, Guleria V. Integrative computational approaches for discovery and evaluation of lead compound for drug design. Frontiers in Drug Discovery. 2024 Apr 5; 4:1362456.
33. Rehman AU, Khurshid B, Ali Y, Rasheed S, Wadood A, Ng HL, Chen HF, Wei Z, Luo R, Zhang J. Computational approaches for the design of modulators targeting protein-protein interactions. Expert opinion on drug discovery. 2023 Mar 4;18(3):315-33.
34. Çevik UA, Işik A, Karakaya A. ADMET and Physicochemical Assessments in Drug Design. Computational Methods for Rational Drug Design. 2025 Jan 20:123-51.
35. Ancuceanu R, Lascu BE, Drăgănescu D, Dinu M. In silico ADME methods used in the evaluation of natural products. Pharmaceutics. 2025 Jul 31;17(8):1002.
36. Wang Y, Xing J, Xu Y, Zhou N, Peng J, Xiong Z, Liu X, Luo X, Luo C, Chen K, Zheng M. In silico ADME/T modelling for rational drug design. Quarterly reviews of biophysics. 2015 Nov;48(4):488-515.
37. Sucharitha P, Reddy KR, Satyanarayana SV, Garg T. Absorption, distribution, metabolism, excretion, and toxicity assessment of drugs using computational tools. In Computational approaches for novel therapeutic and diagnostic designing to mitigate SARS-CoV-2 infection 2022 Jan 1 (pp. 335-355). Academic Press.
38. Misra DP, Jain N, Ora M, Singh K, Agarwal V, Sharma A. Outcome measures and biomarkers for disease assessment in Takayasu arteritis. Diagnostics. 2022 Oct 21;12(10):2565.
39. Sawalha AH, Misra DP, Goel R, Alibaz-Oner F, Quinn KA, Grayson PC, Direskeneli H. Advances in the pathophysiology, diagnosis and treatment of Takayasu arteritis. Nature Reviews Rheumatology. 2025 Nov 6:1-5.
40. Dai X, Wang J, Zhang X, Wang L, Wu S, Chen H, Sun Y, Ma L, Ma L, Kong X, Jiang L. Biomarker Changes and Molecular Signatures Associated with Takayasu Arteritis Following Treatment with Glucocorticoids and Tofacitinib. Journal of Inflammation Research. 2022 Jan 1:4395-407.
41. Peremans L, Twilt M, Benseler SM, Grisaru S, Kirton A, Myers KA, Hamiwka L. Real-World Biomarkers for Pediatric Takayasu Arteritis. International Journal of Molecular Sciences. 2024 Jul 4;25(13):7345.
42. Ihim SA, Abubakar SD, Zian Z, Sasaki T, Saffarioun M, Maleknia S, Azizi G. Interleukin-18 cytokine in immunity, inflammation, and autoimmunity: Biological role in induction, regulation, and treatment. Frontiers in immunology. 2022 Aug 11; 13:919973.

43. Wolosowicz M, Prokopiuk S, Kaminski TW. Matrix Metalloproteinase-9 (MMP-9) as a Therapeutic Target: Insights into Molecular Pathways and Clinical Applications. Pharmaceutics. 2025 Nov 4;17(11):1425.
44. Caselli C, Di Giorgi N, Ragusa R, Lorenzoni V, Smit J, El Mahdiui M, Buechel RR, Teresinska A, Pizzi MN, Roque A, Poddighe R. Association of MMP9 with adverse features of plaque progression and residual inflammatory risk in patients with chronic coronary syndrome (CCS). Vascular Pharmacology. 2022 Oct 1; 146:107098.
45. Misra DP, Singh K, Sharma A, Agarwal V. Arterial wall fibrosis in Takayasu arteritis and its potential for therapeutic modulation. Frontiers in Immunology. 2023 May 15; 14:1174249.
46. Wen D, Feng L, Du X, Dong JZ, Ma CS. Biomarkers in Takayasu arteritis. International Journal of Cardiology. 2023 Jan 15; 371:413-7.
47. Danda D, Goel R, Kabeerdoss J, Sun C, Danda S, Lincy Franklin A, Joseph G, Nath SK. Angiogenesis related genes in Takayasu Arteritis (TAK): robust association with Tag SNPs of IL-18 and FGF-2 in a South Asian Cohort. Journal of Human Genetics. 2024 Jan;69(1):13-8.
48. Alibaz-Oner FA, Yentür SP, Saruhan-Direskeneli G, Direskeneli H. Serum cytokine profiles in Takayasu's arteritis: search for biomarkers. Clin Exp Rheumatol. 2015 Mar 1;33(2 Suppl 89):32-5.
49. Kouranov A, Xie L, de la Cruz J, Chen L, Westbrook J, Bourne PE, Berman HM. The RCSB PDB information portal for structural genomics. Nucleic acids research. 2006 Jan 1;34(suppl_1): D302-5.
50. Trott O, Olson AJ. AutoDock Vina: improving the speed and accuracy of docking with a new scoring function, efficient optimization, and multithreading. Journal of computational chemistry. 2010 Jan 30;31(2):455-61.
51. Kim S, Thiessen PA, Bolton EE, Chen J, Fu G, Gindulyte A, Han L, He J, He S, Shoemaker BA, Wang J. PubChem substance and compound databases. Nucleic acids research. 2016 Jan 4;44(D1): D1202-13.
52. Baroroh U, Biotek M, Muscifa ZS, Destiarani W, Rohmatullah FG, Yusuf M. Molecular interaction analysis and visualization of protein-ligand docking using Biovia Discovery Studio Visualizer. Indonesian Journal of Computational Biology (IJCB). 2023 Jul 21;2(1):22-30.
53. Pettersen EF, Goddard TD, Huang CC, Couch GS, Greenblatt DM, Meng EC, Ferrin TE. UCSF Chimera—a visualization system for exploratory research and analysis. Journal of computational chemistry. 2004 Oct;25(13):1605-12.
54. Daina A, Michielin O, Zoete V. SwissADME: a free web tool to evaluate pharmacokinetics, drug-likeness and medicinal chemistry friendliness of small molecules. Scientific reports. 2017 Mar 3;7(1):42717.
55. Tian W, Chen C, Lei X, Zhao J, Liang J. CASTp 3.0: computed atlas of surface topography of proteins. Nucleic acids research. 2018 Jul 2;46(W1): W363-7.